

Prototype of a DIRC-barrel for the $\bar{\text{P}}\text{ANDA}$ Experiment

Roland Hohler, Dorothee Lehmann, Klaus Peters, Georg Schepers, Carsten Schwarz, Concettina Sfienti, Wolfgang König, Marek Palka, Michael Traxler

Abstract—The $\bar{\text{P}}\text{ANDA}$ Experiment will be one of the large experiments of the future FAIR facility. The physics program requires a good kaon/pion-separation. To achieve this goal, three Cherenkov detectors are foreseen. Around the interaction point a DIRC-barrel is planned with a readout-box inside the magnetic field. A radiator quality test is shown to point out the importance of the knowledge of the radiator surface roughness. The precision of the roughness determination itself is better than 2Å . Furthermore the first prototype of a DIRC-barrel is presented in detail. The focussing readout is realized by a lens, attached at the end of the radiator. As photon detectors micro-channel plate PMTs are used to fulfill the requirement of an magnetic-insensitive detection. Finally preliminary results of a recent test with 2.3 GeV protons show the successful measurement of Cherenkov ring fragments in the expected region.

I. INTRODUCTION

THE $\bar{\text{P}}\text{ANDA}$ Experiment (AntiProton Annihilations at Darmstadt) shown in Fig. 1 is an universal detector for strong interaction studies and will be located at the high-energy storage ring HESR at the international Facility for Antiproton Ion Research (FAIR). The provided beam of antiprotons in the energy range of $1\text{--}15\text{ GeV}$ is of unprecedented intensity, so that the detector will be an excellent tool for a better comprehension of the Quantum Chromo Dynamics. For the physics analyses it is crucial to have a kaon/pion PID (particle identification) [1]. Therefore three Cherenkov counters are arranged to cover a large solid angle. One of these is arranged as a barrel around the interaction point. The barrel covers an polar angle from 22 to 120° . Particles in this angular region are relatively slow, so that solid state radiators are necessary with higher refraction indices. Furthermore the radial space is limited because of the outside following electromagnetic calorimeter. On that account we chose for the Cherenkov detector in the barrel section a DIRC (Detection of Internally Reflected Cherenkov light) detector. Due to the desired compactness of the $\bar{\text{P}}\text{ANDA}$ detector the readout volume of the barrel-DIRC is planned to be inside the magnetic field. The radiator geometry is a thin bar with a rectangular cross section. As material one commonly uses quartz (synthetic fused silica) because of its irradiation hardness, long attenuation length for photons and high refraction index [2]. The lower momentum threshold of kaons producing Cherenkov light is about 440 MeV for that material.

Manuscript submitted November 14, 2008.

All authors are with the GSI Helmholtzzentrum für Schwerionenforschung GmbH. R. Hohler and K. Peters are additionally with the Goethe University Frankfurt.

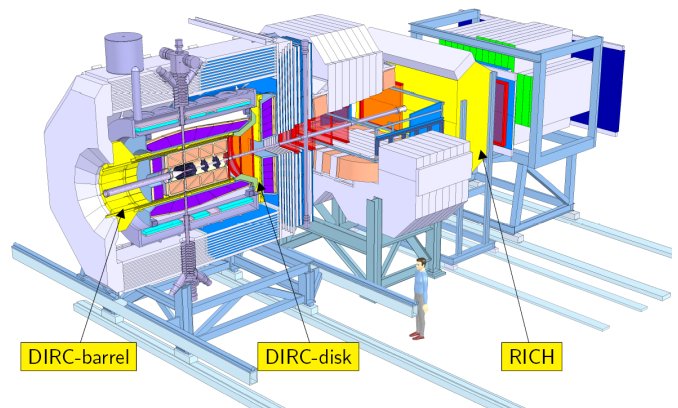


Figure 1. Preliminary setup of the $\bar{\text{P}}\text{ANDA}$ detector. The three foreseen Cherenkov detectors are highlighted in yellow.

The DIRC-concept is based on the photon propagation in the radiator by total internal reflection. A charged particle with superluminal velocity in the radiator material generates Cherenkov photons along the particle trajectory through the radiator. A fraction of these photons fulfill the total internal reflection constraint and are reflected several hundred times before exiting the radiator. Photons which originally propagate away from the readout volume are reflected back by a mirror at the end of the radiator. Since the radiator cross section is rectangular, the Cherenkov cone angle is preserved for each reflection. An optical coupling medium between radiator bars and photon detectors reduces distortion effects. For the $\bar{\text{P}}\text{ANDA}$ DIRC-barrel this coupling medium will be index-matching oil like Marcol [3][4]. Due to the numerous reflections the photon detectors do not measure a Cherenkov ring like with a RICH detector but rather parts of this ring. By reconstructing these ring fragments a particle identification can be carried out.

An additional feature of the $\bar{\text{P}}\text{ANDA}$ DIRC-barrel will be the measurement of the time of propagation (TOP). By measuring the relative time differences of the incident photons on the photon detectors, it is possible to reconstruct the time of propagation and, with the spatial information of the ring fragment, to determine the wavelength of the photon for dispersion corrections. Thereby the DIRC-barrel will be a novel 3D-DIRC using the two-dimensional space position of a hit in a photon detector pixel and the associated time of the hit. The necessary time resolution should be better than 0.5 ns favoring photon detectors like a micro-channel plate PMT.

II. RADIATOR QUALITY TEST

IN spite of the total internal reflection the reflection loss depends on the surface roughness of the radiator. The probability of the reflection loss ($1 - \mathcal{R}$) for a single reflection is in the range of per mille. The total reflection loss is defined as $1 - \mathcal{R}^N$ whereas N is the number of internal reflections inside the radiator. Later in the experiment the expected number of reflections is in the order of 100 and hence the loss is not anymore negligible. Furthermore the obtained photon statistics is low because only some hundreds of Cherenkov photons per particle are generated in the detectable wavelength range and only a part of them are transported through the bar.

Unfortunately we have not the possibility to measure directly the roughness of the radiator. But the scattering theory provides a relationship between reflection loss and roughness [5][6]:

$$1 - \mathcal{R} \approx \left(\frac{4\pi \cdot \sigma \cdot \cos(\Theta)}{\lambda} \right)^2 \quad \text{for } \sigma \ll \lambda \quad (1)$$

in which Θ is the incidence angle and λ the wavelength of the photon. For the definition of the roughness one assumes a normally distributed surface with RMS-roughness σ . Since the reflection loss in the quartz bar should be as low as possible, the roughness will be in the range of 0-100 Å and therefore it is smaller than the photon wavelength. Fig. 2 shows the single reflection loss in dependency on the wavelength for different roughness values. With this theory we are able to check the roughness specification from the manufacturer.

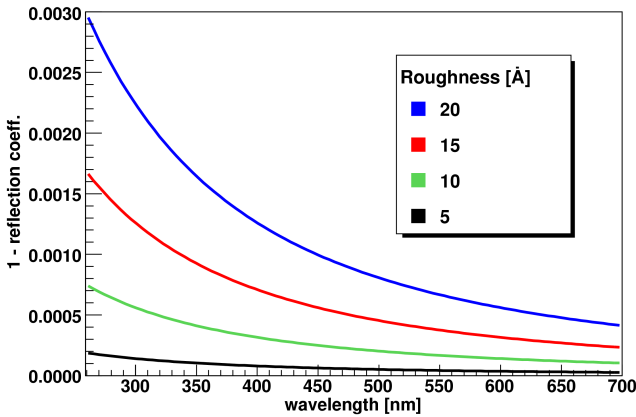


Figure 2. Theoretical relationship between single reflection loss and different roughnesses depending on the photon wavelength.

A. Internal reflection setup

The experimental setup is designed to precisely study the optical properties of the quartz bar including bulk attenuation and reflection coefficient \mathcal{R} . Both quantities are measured by a transmission measurement. The schematic in Fig. 3 shows the setup to determine the single reflection probability \mathcal{R} . The setup for the bulk attenuation determination is quite the same but without internal reflection inside the radiator.

To simulate the Cherenkov photons we use diode-pumped solid state lasers with

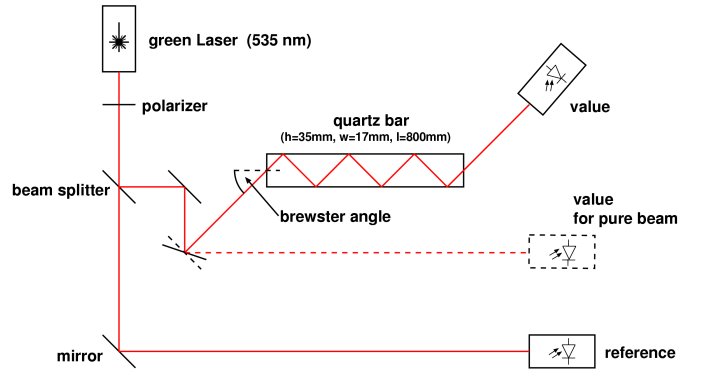


Figure 3. Experimental setup to measure the transmission of the beam propagating via total internal reflection through a quartz bar.

different wavelengths. For a start a green laser (535 nm) is applied. A beam splitter provides the beam for two photodiodes (Hamamatsu S1723-06) [7]. One of both is used as a reference to cancel out laser intensity fluctuations. To avoid reflection loss at the front surface of the quartz bar we couple in linearly polarized laser at the Brewster angle. The artificial fused silica bar is 800 mm long, 35 mm wide and 17 mm high. The quartz glass grade is Lithosil[®] Q0 from the manufacturer Schott Lithotec [8]. The photodiodes are operated unbiased in the photovoltaic mode because of the good linear response and the negligible dark current [9]. The readout circuit of these diodes acts as a current to voltage converter and is connected to an ADC. To calculate the transmission T , the intensity ratios R , measured by both diodes, for with quartz bar and pure beam have to be determined before (see also Fig. 3):

$$T = \frac{R_{quartz}}{R_{pure}} \quad \text{with } R = \frac{V_{val}}{V_{ref}}.$$

Finally the whole setup is installed in a dark box protected from external influences such as daylight, thermal fluctuations and dirt.

B. Roughness determination

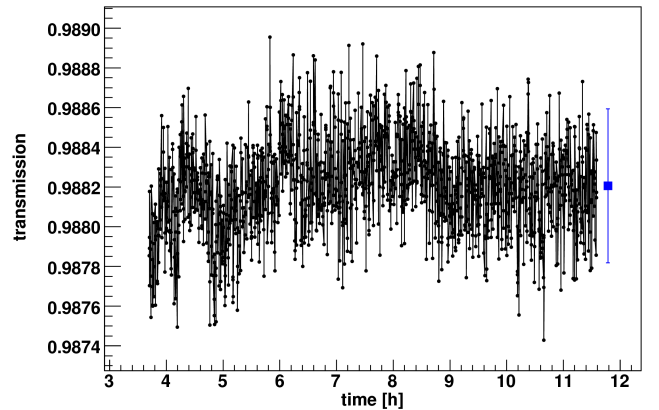


Figure 4. Eight hours long transmission measurement for the determination of the reflection coefficient. In blue the average transmission value.

A transmission measurement with the previously presented setup is shown in Fig. 4. The measurement duration was about eight hours to check the stability and drift of the transmission value for example due to temperature changes. In this time the fluctuations of the transmission value were about of 1.5%. The average transmission shows a precision better than a half per mille:

$$T = 0.9882 \pm 0.0004.$$

It depends on the reflection coefficient \mathcal{R} and the bulk attenuation,

$$T = \mathcal{R}^N \cdot \exp\left(-\frac{L}{\Lambda}\right), \quad (2)$$

with N the number of internal reflection inside the quartz bar, Λ the attenuation length of fused silica and L the optical pathlength of the laser beam. Its pathlength can be estimated by [10]

$$L = l \cdot \sqrt{1 + \left(\frac{b \cdot N}{l}\right)^2},$$

in which l is the length and b the width of the fused silica bar. This yields for the attenuation a value of

$$\Lambda = (281 \pm 97) \text{ m} \quad \text{for} \quad 535 \text{ nm}.$$

The origin of this large uncertainty comes from the shortness of the quartz bar which is much smaller than the to measured attenuation length. BaBar measured $(500 \pm 167) \text{ m}$ at 442 nm [10]. Assuming Rayleigh scattering ($\Lambda \sim \lambda^4$), which is general the dominated attenuation contribution, the scaled attenuation length for a wavelength of 535 nm accounts to $(1073 \pm 359) \text{ m}$. This value is almost four times greater than our result but the contribution of the attenuation length to the transmission is only in the order of per mille.

The observed number of reflections inside the quartz bar is $N = 15$. With the measured quantities needed in equation (2) one can extract the reflection coefficient and hence the single reflection loss:

$$\begin{aligned} \mathcal{R} &= 0.99944 \pm 0.00009 \\ 1 - \mathcal{R} &= 0.00056 \pm 0.00009. \end{aligned}$$

With equation (1) the corresponded roughness is

$$\sigma = (17.8 \pm 1.5) \text{ \AA}$$

which is close to the specification from the manufacturer of 20 Å.

III. DIRC-BARREL PROTOTYPE

To study the performance of our DIRC-barrel prototype a test with a proton beam at GSI was performed. The main goal of the experiment was to see and to identify Cherenkov photons. Before, the whole setup was tested extensively by measuring cosmics. Also tests concerning the readout volume including the photon detectors were carried out.

A. Focussing readout

The purpose of having a focussing DIRC is to achieve a relative compact readout volume. The focussing itself is realized by a lens and by positioning photon detectors in the focal plane. A solution using focussing mirrors is challenging due to the space requirements.

For a better comparison between focussed and unfocussed scenario, the simulation results of an unfocussed prototype are shown in Fig. 5. The setup is realized by a box filled with oil to avoid optical image distortions, attached at the quartz bar. In the simulation it was assumed that the refraction index of the oil is the same as for fused silica. At the end of the box photon detectors are mounted. The distance between bar and detector is 23 cm. It was simulated that a particle close to the Cherenkov threshold of $\beta = 0.7$ travels centered through the bar in the detector direction. The Cherenkov cone angle is about 13° . For sufficient statistics 5000 photons were generated. The simulation plot shows the expected smeared Cherenkov ring which is not symmetric because of the rectangular cross section of the quartz bar. Due to the preferred simulated Cherenkov cone axis, which is parallel to the bar, the ring is continuous and hence no ring fragments are observable as usually expected in a DIRC.

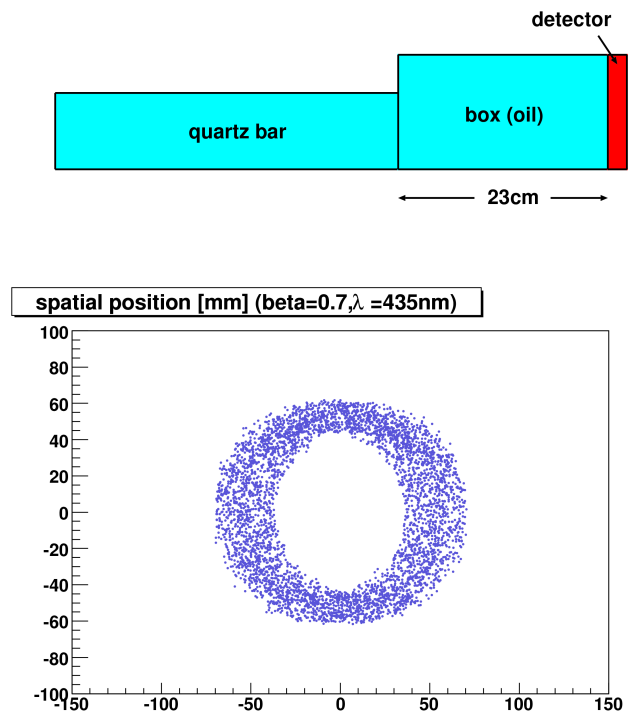


Figure 5. Setup of the unfocussed readout and the simulated Cherenkov ring for a certain wavelength on the detector.

The focussing readout is realized by a spheric lens with a focal length of $f_{lens} = 15 \text{ cm}$, attached at the exit of the bar (Fig. 6). For a continuous transition between bar and lens, oil is used as coupling material. The refraction index of the lens matches that of quartz. After the lens there is an air-gap. Apart from that the setup is the same as for the unfocussed scenario. The whole setup can also be seen as a diverging

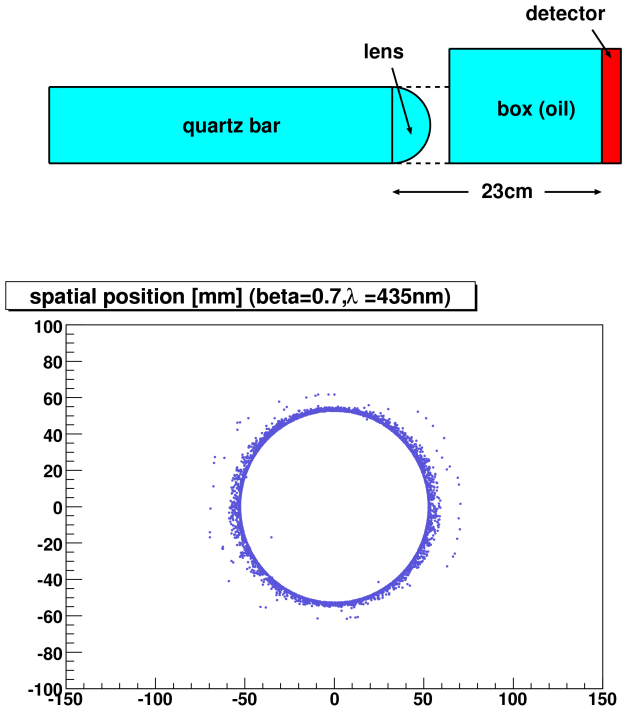


Figure 6. Setup of the focussing readout and the simulated Cherenkov ring of a certain wavelength. The dashed lines around the air-gap between lens and box indicate the resultant air-lens.

air-lens, and the environmental medium is fused silica. Since the refractivity for air is lower than for quartz, the divergent air-lens works as a converging lens. The focal length with oil in the box is:

$$f_{air-lens} = f_{lens} \cdot n_{oil} \approx 22 \text{ cm for } 435 \text{ nm.}$$

The simulated Cherenkov ring is now sharp. The small smearing comes from the lens aberrations. It is also asymmetric as explained for the unfocussed case. This focus effect using only one lens can only be achieved for a small wavelength bandwidth. Generating the whole detectable Cherenkov spectrum, the dispersion effects will smear the simulated ring in such a way that the difference will be hardly visible.

Later in the PANDA experiment a system of lenses will be used to correct lens aberrations and dispersion effects and for obtaining a flat focal plane. The R&D for that is in progress.

B. Photon detector

For our first prototype we decided to choose the microchannel-plate-PMTs (MCPs). A big advantage of using MCPs compared to the standard vacuum PMTs is their magnetic insensitivity to fields up to 2 T which is a requirement for the photon detectors in the PANDA experiment [11]. In addition to that MCPs have a transient time spread (TTS) better than 50 ps. This good time resolution is very important for the time of propagation measurement. On the other hand a caveat using MCPs later in the experiment is its short lifetime.

C. Test with protons

The beam time took place recently at the GSI in Darmstadt with 2.3 GeV proton beam which corresponds a velocity of $\beta = 0.9571$.

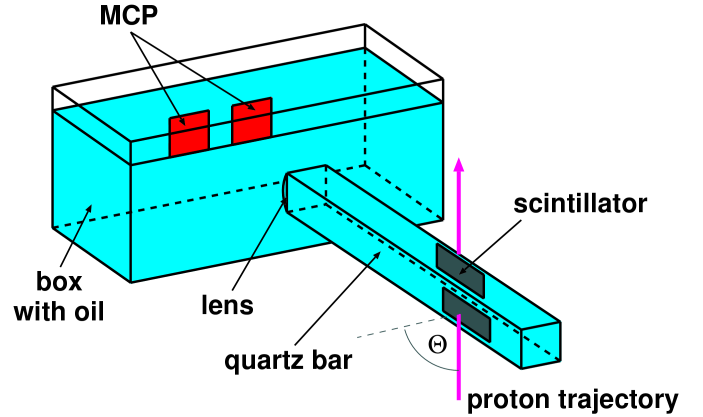


Figure 7. Schematic setup of the beam test.

1) *Test setup:* The setup (Fig. 7) is the same as described in section III-A for the focussed case and is installed in a light-tight box:

- a fused silica bar, with the same dimensions and surface quality used in the radiator quality test (section II)
- a spheric lens with a focal length of 15 cm at the end of the bar
- a fishtank with a width of 20 cm and a length of 30 cm filled with pump oil
- two 8×8 pixel MCPs (Burle 85011-501) with an active area of $51 \times 51 \text{ mm}^2$ [12] installed in a distance of 23 cm from the bar end.

The proton beam hits the bar with an angle of 57° and traverses two $3 \times 3 \text{ cm}^2$ sized scintillator paddles acting as a coincidence trigger. The MCP supply voltage is 2.4 kV. For all pixel of a MCP, the discriminators were set uniformly to 20 mV. The single photon signal is about 50 mV after all preamplification stages. The data acquisition is carried out by the HADES trigger and readout board (TRBv2) [13].

2) *Preliminary results:* Fig. 8 shows the simulation of the expected Cherenkov ring fragments on the focal plane. The colors of the markers correspond with the photon wavelength whereas for the ultraviolet range grey is used. The ring structure shows gaps which comes from the internal reflection in the radiator. Furthermore the position for the two MCPs are drawn.

By now only a fraction of the total recorded dataset was preliminary analyzed. In Fig. 9 the used dataset is about 5%. The color code of the registered hits by the MCPs is in a logarithmic scale. Both MCPs show an accumulation of hits on one half of their sensitive area after a time-cut to reduce noise. Due to this count statistics we can identify the hits as Cherenkov photons. Simulation and data are in agreement. Nevertheless both, data and prototype performances, have to be analyzed more carefully. Unclear is for example in the data the lack of the gaps in the ring structure exhibited by the simulation. Probably the smearing effect by different refraction

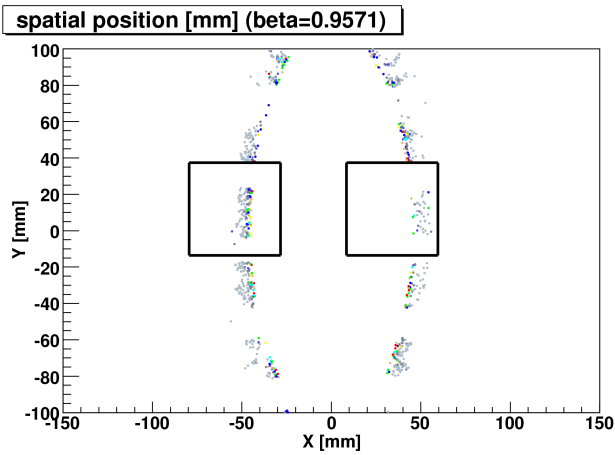


Figure 8. Simulation of the expected Cherenkov ring fragment on the rear side of the box and the position of the two MCPs on that.

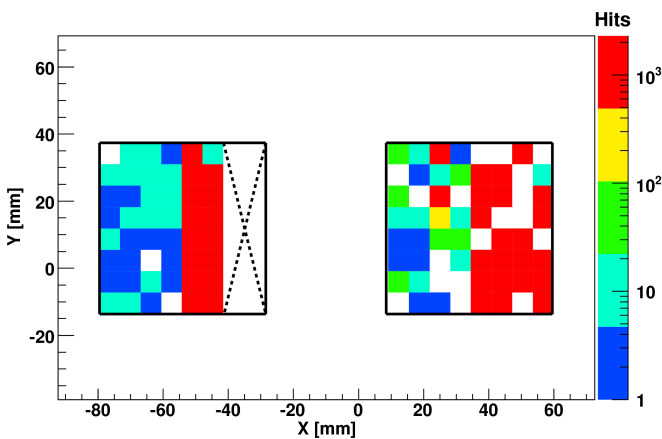


Figure 9. Hits on the two MCPs with 5% of the dataset. Color code is in a logarithmic scale.

indexes of lens and oil compared to quartz is larger. Moreover the electronics associated with some pixel was not working properly during the beam time. In order to address these and other issues a laser calibration of the whole setup with LED is currently ongoing and for the next beam time in spring or summer 2009 it is planned to cover a larger area of the screen by using at least four MCPs.

IV. CONCLUSION

The presented results in this paper show the progress of the R&D and quality assurance of the DIRC-barrel for the future project PANDA at FAIR. One of the tasks in the radiator quality test is the investigation of the radiator surface. For that a transmission precision much better than 1% was achieved. This enables to determine the quartz bar roughness with an uncertainty better than 2 \AA . For the first prototype the focussing readout is realized by a lens and followed by a small air-gap. This gap allows a simpler integration of the photon detectors in the complete setup. As photon detector we decide to choose MCPs because of its insensitivity to a magnetic field which is a requirement for the DIRC in the PANDA detector. A test with protons for the prototype was

performed. Cherenkov ring fragments were measured and the experimental results and the simulation are in agreement. Since the presented results of this test are preliminary and only a fraction of the total dataset was used, full detailed analyzes are in progress.

ACKNOWLEDGMENT

This work is supported by EU FP6 grant, contract number 515873, DIRACsecondary-Beams.

Also thanks to the CBM Collaboration that we could participate to their beam time getting a parasitic beam and hence for testing our prototype in a more "real-experiment" environment.

REFERENCES

- [1] PANDA Collaboration *Technical Progress Report of PANDA: Strong Interaction Studies with Antiprotons* 2005.
- [2] BaBar collaboration *The DIRC Particle Identification System for the BaBar Experiment* SLAC-PUB-10516.
- [3] ExxonMobil Oil Corporation, <http://www.exxonmobil.com/>
- [4] B. Brown et al. *Study of scintillation, fluorescence and scattering in mineral oil for the MiniBooNE neutrino detector* IEEE NSS Conference Record, 2004.
- [5] P. Beckmann and A. Spizzichino, *The scattering of electromagnetic waves from rough surfaces* Pergamon Press, 1963.
- [6] J. Elson, H. Bennett and J. Bennett, *Applied Optics and Optical Engineering Vol. VII, Chapter 7* Academic Press, 1979.
- [7] Hamamatsu Photonics, <http://www.hamamatsu.com/>
- [8] Schott Lithotec AG, <http://www.schott.com/lithotec/>
- [9] W. Kester, S. Wurcer, C. Kitchin *Sensor Signal Conditioning, Section 5: High Impedance Sensors* Analog Devices Inc.
- [10] J. Cohen-Tanugi et al. *Optical properties of the DIRC fused silica Cherenkov radiator* NIM A 515 (2003) 680-700.
- [11] provided by A. Lehmann University Erlangen.
- [12] Photonis/Burle Industries Inc., <http://www.burle/>
- [13] M. Traxler et al. *A general purpose Trigger and Readout board (TRB) for HADES and FAIR-Experiments* GSI Scientific Report, 2006.